CHALMERS

Feasibility of fetal EEG Recording

during labor by using STAN S31

Farhad ABTAHI

Supervisor: Professor Kaj Lindecrantz

Co-Supervisor: Dr. Nils Lofgren

Examiner: Professor Bo Håkansson

Department of Signal and System
CHALMERS UNIVERSITY OF TECHNOLOGY
Gothenburg, Sweden 2011
Master's Thesis EX101/2011

Feasibility of fetal EEG recording during labor by using STAN S31

Master's Thesis EX101/2011

Department of Signal and System
Chalmers University of Technology
SE-41296 Göteborg
Sweden

Tel. +46-(0)31 772 1000

Prepared With LaTeX
Reproservice / Department of Signal and System
Göteborg, Sweden 2011

Abstract

Fetal electrocardiography is currently used for monitoring of fetus during labor. ST-Analysis is done by monitoring amplitude of T wave to find elevation of ST wave amplitude which is a sign of hypoxia. The ST-Analysis in combination of standard cardiotocography (CTG) helps finding general ischemia due to specific fetal positioning that chokes the umbilical cord. The fetal electrocardiogram signals obtain by placing electrode on fetal scalp during labor (after water breaks) referred to an electrode on the mother's thigh. The STAN S31 is an apparatus which is use for intra-partum fetal monitoring. This method is currently used with great success in majority of Swedish hospitals and in 80 to 90 percent of labor and delivery clinics in Norway, Belgium and Denmark. The purpose of this project is to study feasibility of extracting brain waves from recording signals. The fetal EEG could be used to improve monitoring in cases were the fetus is too exhausted to respond with T amplitude elevation or when monitoring is started too late and hence T amplitude elevation has already occurred and relative measures are useless.

During this study, amplifier modifications were done to achieve 1 μV resolution. The modified STAN device is used for recording in the delivery department of Sahlgrenska University Hospital, Mölndal. Two ECG elimination methods are implemented; ensemble average subtraction and wavelet denoising methods. Comparison of these methods has been done by use of simulated and real signals. The result shows successfully elimination of ECG artifacts. However, by using the ensemble average subtraction method some attenuated QRS are still visible. It is also concluded that ensemble average subtraction behaves like a high-pass filter while wavelet denoising method acts as low-pass filter. The preference of each method depends on the application.

The remained signals after eliminating ECG have time and frequency patterns similar to EEG. However, the lack of sufficient eventful recordings and limits in frequency range of high resolution channel makes the final decision about existence of EEG signals impossible. The final judgment needs future investigation to improve the frequency range of the signals and to correlate the potential EEG signals to somatosensory evoked potentials or other events.

Keywords: Fetal Monitoring, Fetal ECG, Fetal EEG, EEG Noise Reduction, Wavelet Denoising, Ensemble Average Subtraction, STAN S31

Acknowledgments

I am very grateful for the help and support of my supervisor, Professor Kaj Lindecrantz. Also special thanks to my co-supervisor Dr. Nils Löfgren, who always was available for project with his valuable time. This work have not been possible without help of associate Professor. Magnus Thordstein who did visual analysis of signals and pushed the project. The big thanks to Dr. Johan Lofhede who share his place with me. Finally, I would also like to thank Shirin for her love and patience with me. I am also very grateful to my family for their long-distance support.

Farhad Abtahi, Göteborg 2011

Contents

List of Figures

List of Tables

1

Introduction

Todays, the fetal electrocardiography is widely using for monitoring the fetus during labor, it can use to find general ischemia due to specific fetal positioning that chokes the umbilical cord. The noninvasive fetal electrocardiography which records from maternal abdomen is contaminated with different noises like maternal ECG, fetal brain activity; myographic (muscle) signals from both mother and fetus, movement artifacts and multiple layers of different dielectric biological media through which electrical signals are pass. The figure 1.1 illustrates different medias that influence surface potentials. The development of signal processing techniques like adaptive filtering and array signal processing make it possible to cancel maternal cardiac interference. However, these methods never provide more than approximate of fetal heart rate and fECG analysis is still challenging biological signal processing problem. Noninvasive fetal cardiac monitoring methods today are based on fetal heart rate which does not include characteristics of fECG. The invasive fECG recording by placing electrode on fetal scalp during labor is the only reliable fECG measurement method now. [1]

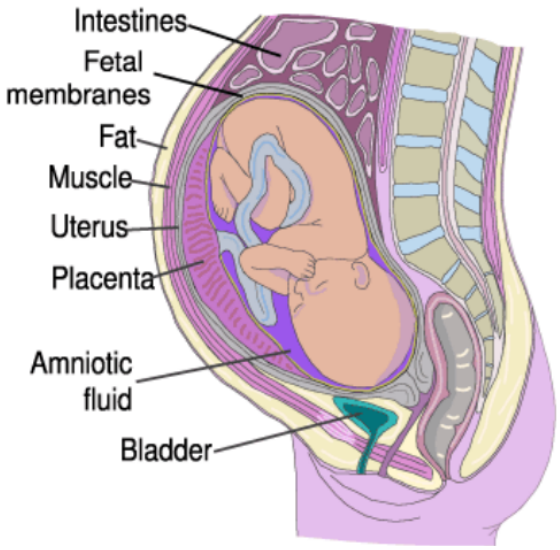

Figure 1.1: The major medias which influence the fetal cardiac surface potentials [1]

The Neoventa Medical AB is a company in Gothenburg with subsidiaries in Boston, USA and Paris, France. The company is provider of fetal monitoring solutions and services that improve obstetric care. The Neoventa solution is called STAN which combine standard cardiotocography (CTG) with ST-Analysis. The CTG is a technical term for recording fetal heartbeat and uterine contraction during pregnancy. The ST-Analysis will inform the care staffs in case of ST wave amplitude elevation which is the sign of hypoxia. This method is currently used with great success in majority of Swedish hospitals and in 80 to 90 percent of labor and delivery clinics in Norway, Belgium and Denmark. The Stan S31 monitoring system is presented in figure 1.2.

Figure 1.2: STAN S31 and it's usage in hospital

The fECG signals currently records from electrode placed on fetus scalp with reference of electrode on mother tight. The STAN S31 today uses a 12 bit analogue to digital converter which gives a 5 μV resolution and dynamic window of $+/-10V$. The improvement of resolution in next generation of STAN monitors can provide opportunities for more precise monitoring of heart rate and more accurate ECG shape analysis and possibly additional features.

1.1 Objective

The aim of this project is to study possibility of extracting brain waves from recording signals. The fetal EEG could use to improve monitoring in cases were the fetus is too exhausted to respond with T amplitude elevation or when monitoring start too late. Therefore, T amplitude has already occurred and relative measures are useless.
The project objectives are divided as below:

- Perform a literature study
- Hardware modification on STAN S31 to achieve 1 μV resolution
- Record signals from STAN with a resolution of 1 μV
- Implement suitable algorithms in MATLAB to filter out the ECG from the Fetal Heart Rate (FHR) lead signal
- In collaboration with a neurophysiologist, determine if the remaining signals contain clinically relevant EEG

1.2 Outline

At the beginning an overview over the basic principles of fetal electrocardiogram(fECG) and fetal electroencephalogram for medical application will provide the background knowledge about project in chapter 2. The current amplifier of STAN 31, available channels, limitations and modification which has done to improve resolution are discussed in chapter 3.3. Chapter 4 contains recording protocol, preprocessing, implemented R-Peak detection and ECG rejection algorithms. Chapter 5 is concerned with the results. Chapter 6 includes discussion about current results. Chapter 7 is mentioned the final conclusions. Finally, in chapter 8 the possible future work is described.

2

Background

2.1 Cardiovascular system

The circulatory system consists of heart, blood vessels and blood. The heart is divided into right and left part, each consisting of an atrium and a ventricle. The blood flows through whole body by pressure created by pumping action of the heart. The cardiovascular system forms a closed loop of two circuits; pulmonary and systemic. The blood pumps from the right ventricle through the lungs and then to the left atrium, it is called pulmonary circulation. The blood then pumps from left ventricle through the systemic circulations to all organs and tissues of the body except lungs and the right atrium. [2]

2.1.1 Heart Activities

The efficient pumping of blood requires well-ordered contraction of arterials and ventricles. The atria contract first and then immediately ventricles will contract. The contraction of cardiac muscle is triggered by depolarization of the plasma membrane. The conducting system of heart is depicted in figure 2.1. The initial depolarization arises in sinoatrial (SA) node which is located in the right atrium. The SA node discharge rate controls the heart rate. The depolarization first spreads to atrial muscles and conduction is fast enough in order to left and right atria contract at the same time. The depolarization will conduct to ventricles through ventricular (AV) node which is located in the base of right atrium. After the AV node, the pulse enters bundle of Hiss which is located between walls of two ventricles. Since the atria completely separated from ventricles by layer of nonconducting tissue, the bundle of His is the only electrical conduction between atria and ventricles. The bundle of His will divide to right and left bundle branches and make contact with Purkinje fibers which finally make contact with ventricular myocardial cells. The conduction along the Purkinje fibers is very fast and depolarization of all right and left ventricular are more or less simultaneously. However, the conduction and contraction are done slightly earlier in the bottom of the ventricles and it make the contraction more efficient (can compare to squeezing a tube of toothpaste from the bottom). [2]
The normal heart beat include sequence of mechanical and electrical events which are summarized here:

1. Generation of action potential in SA node and spread to both atria.
2. Contraction of both atria
3. The action potential reach the AV node and trigger it
4. The blood will push from the atria to ventricles during the atrial contraction
5. The AV node action potential will spread to the Purknje fibers through bundle of Hiss
6. Both ventricles will contact due to spread of AV action potential; The left ventricle pumps blood to the systemic circulation while the right ventricle supplies the pulmonary system
7. The heart muscles will be relax but blood continues to flow due to elastic recoil of arterial walls

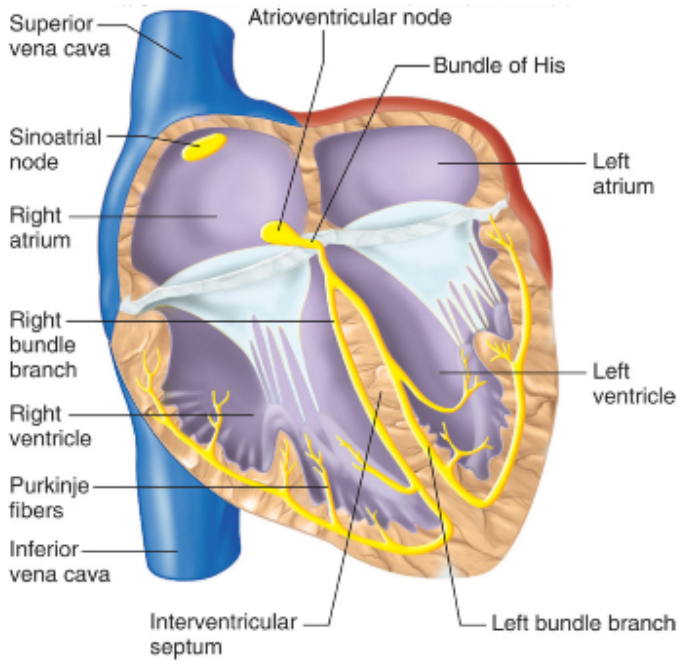

Figure 2.1: The Conducting system of the heart [2]

2.1.2 Fetal vs. Adult Heart

The electrical activity of fetal heart is similar to the adult heart while its mechanical function is different. There are some functional differences between the fetal and adult heart. It is known that the fetal oxygen is supplied by placenta. Therefore, pulmonary circulation is bypass by using two shunts, namely the foramen ovale and ductus arteriosus which links outgoing vessels of booth ventricles. The similar shunt is called ductus venosus, allows blood to bypass the liver. It carries blood with oxygen and nutrients from the umbilical cord straight to the right side of the fetal heart. The formamen ovale closes with the first breath after birth and ductus arteriosus partially closes 10 to 15 hours after birth. The ductus venosus also closes shortly after birth, when umbilical cord cuts and blood flow between mother and fetus stops. [1]

2.1.3 Electrocardiogram

The Electrocardiogram (ECG) is the primary tool for evaluating the heart electrical events. The action potential of cardiac muscles produces a current which generate electrical filed and can be detected by recording electrodes at body surface. The figure 2.2 illustrate the one cycle of ECG waveform.

Table 2.1: ECG waves and intervals

Wave/Interval	Corresponded Heart Activity	Estimated duration
P-Wave	Atrial Depolarization	100 ms
PR interval	Time action potential moves from atria to ventricles	120-200 ms
QRS complex	Ventricular depolarization	60-100 ms
ST interval	Time between ventricular depolarization and re-polarization	120 ms
T-Wave	Ventricular re-polarization	200 ms

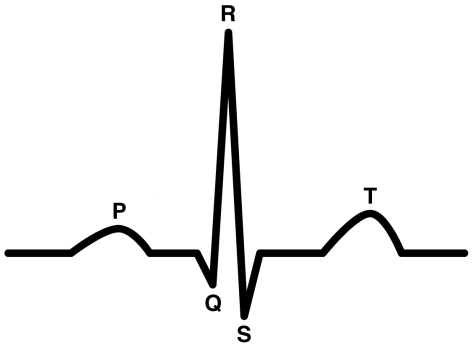

Figure 2.2: The waveform of typical ECG which can record by using skin surface.

The first wave is called P wave and corresponds to the current flows during atrial depolarization. The second deflection, the QRS complex is related to the ventricular depolarization. The final deflection, the T wave is the result of ventricular re-polarization. The atrial re-polarization is absence in ECG due to same timing as QRS. The clinical ECG typically is done by multiple combinations of recording locations on the limbs and chests which calls ECG leads. The shapes and size of the P wave, QRS complex and T wave vary with electrode location. The relation between heart rate activity and ECG waveform and intervals is illustrated in figure 2.3 and is summarized in table 2.1.

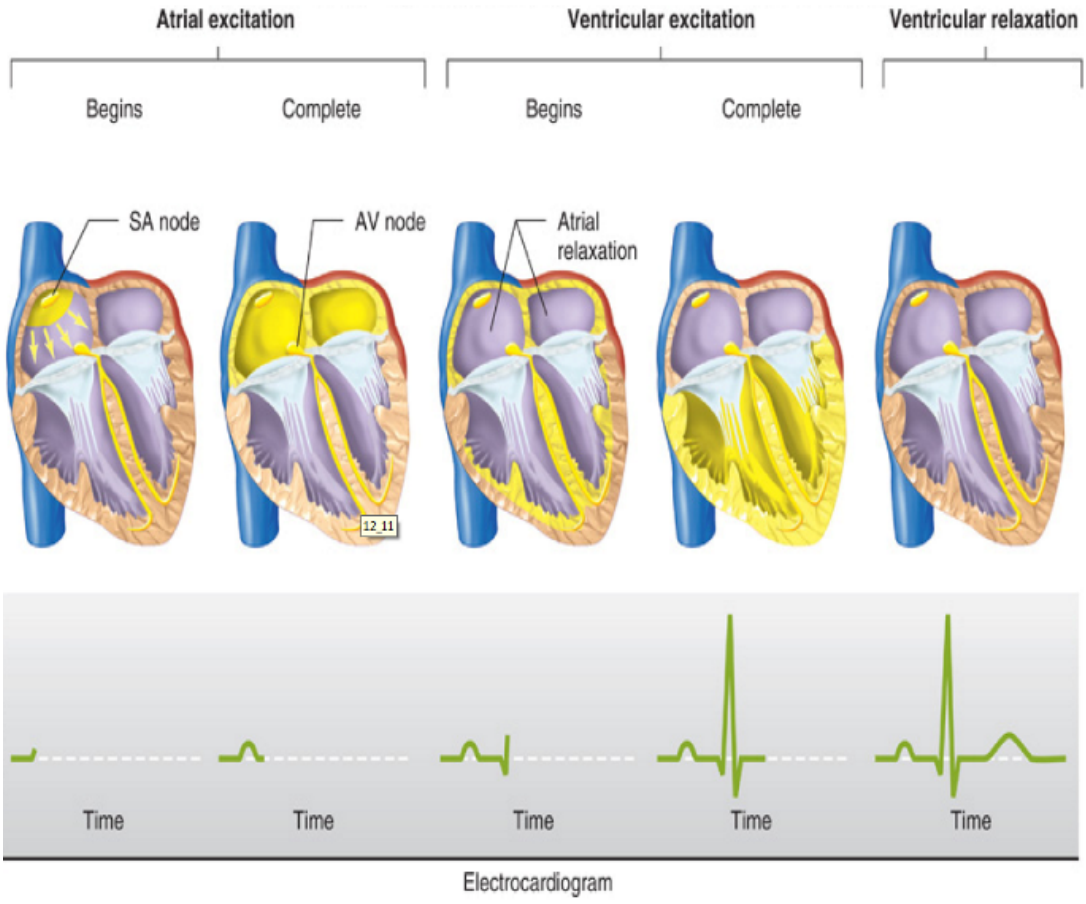

Figure 2.3: The ECG waves compare to the heart electrical activities [2]

2.2 Human Brain

The Central Nervous System (CNS) consists of brain and spinal cord. The brain is the important part of the CNS which is responsible for the control of the body activities. In addition, it is the center of interpretation of information from the senses like sight, hearing, smell etc. The brain has three main parts; the cerebrum, the cerebellum and the brainstem. The cerebrum is the largest portion of the brain and is about the two-third of the total weight of the brain. The thin layer of the cerebrum calls cerebral cortex and it divides into two hemispheres. The right hemisphere controls movements of the left side of the body; the left hemisphere connects to the right side of the body. The cerebral cortex can divide into four sections; the frontal lobe, parietal lobe, occipital lobe and temporal lobe. Different parts of brain and their functions are summarized in figure 2.4 and table 2.2. [2, 3]

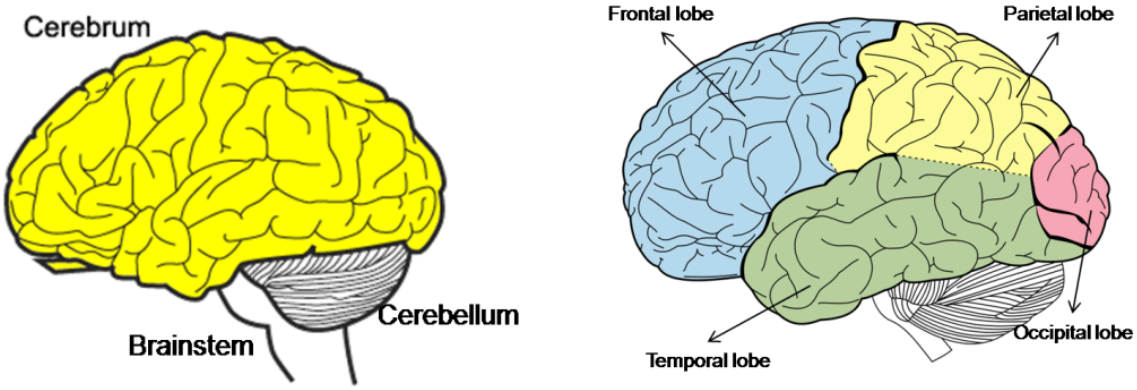

Figure 2.4: Three parts of brain to the left and different lobes of cerebrum to the right [2]

Table 2.2: Functionality of different part of cerebrum [2]

Name	Functions	Position
Frontal Lobe	Reasoning, Motor Skills, high level recognition and expressive language	Front of Brain
Parietal Lobe	Processing of sensory information such as pressure, touch, and pain	Middle Section of Brain
Temporal Lobe	Sounds and Language Interpretation, Formation of memories	Bottom Section of Brain
Occipital Lobe	Interpreting visual stimuli and information	Back portion of Brain

2.2.1 Electroencephalogram

The brain activity can measure with several direct and indirect methods. The imaging methods such as MRI/fMRI, PET/SPET and CAT/CT which measures the brain activity by changes in blood flow, oxygen consumption and glucose utilization are indirect methods. On the other hand, Magnetoencephalograph (MEG) and Electroencephalogram (EEG) are direct methods which measures brain activity by using magnetic and electrical fields. The EEG is a non-invasive brain activity monitoring method which is recorded from electrodes on the scalp and captures the electrical activity of the brain cortex situated in the vicinity of the electrode. The EEG is widely uses because of its non-expensive equipment and devices. Additionally, it can measure with suitable time resolution around 1ms. However, its spatial resolution is not good enough. [2, 3]

The cerebral cortex consists of special neurons called Pyramidal cells which is depicted in figure 2.5. The apex of pyramid is point toward cortical surface while a large dendrite extends further upward to that surface. The axon extends into internal layer (white matter) from the cell body of pyramid. The detailed description of various neurons and layers and functions of brain can be found in [2, 3]. The

synaptic inputs to the apical dendrite tree will depolarize the dendrite membrane. As a result, current flow though pyramidal cell body will produce. The direction of current flow lines shows the cell body behaves as a source (+) while upper apical dendrite tree behaves as a sink (-). Therefore, structure of pyramidal cells can consider as dipole which explains variation of this cortical dipole layer leads to EEG waves. The structure of pyramidal cell as a dipole is depicted in figure 2.5. The EEG recordings are the summation of volume conductor fields produced by millions of interconnecting neurons. However, only synchronous variation in groups of neurons contributes to the EEG signal recorded from scalp surface and asynchronous activity cancels out. [2, 3]

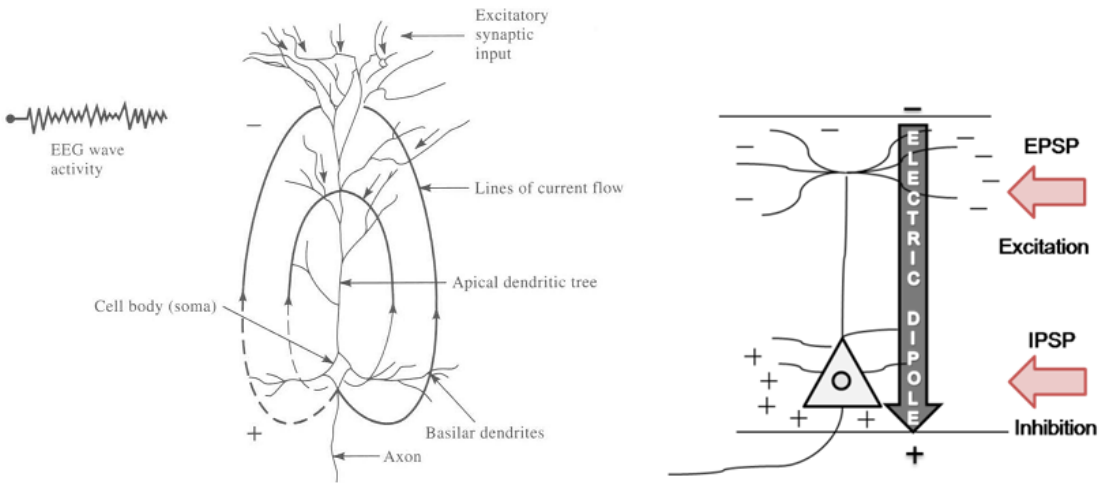

Figure 2.5: The structure of pyramidal cells to the left and electric dipole of pyramidal cells to the right [3]

The EEG signals recorded from scalp can be divided into several frequency bands; Delta Waves (1-3 Hz), Theta Waves (4-7 Hz), Alpha Waves (8-13 Hz), Beta Waves (13-30 Hz and Gamma Waves (30-100 Hz).[3] The samples of brain waves in different bands are depicted in figure 2.6. Delta Waves are high amplitude sinusoidal waves in frequency range of 1-3 Hz and usually known as slow waves. Delta waves are mostly seen during stage N3 (slow wave sleep). Theta Waves are sinusoidal waves in frequency range of 4-7 Hz and usually can be seen during drowsy sleep, light sleep and REM sleep. Alpha waves are recorded during wakefulness with closed eyes on occipital lobe and have oscillations in frequency range of 8-13 Hz. Beta waves usually associated to wakefulness, thinking and active attention and have frequency range of 13-30 Hz.

2.2.2 Fetal Electroencephalogram

The earliest attempt to record human fetal brain activities had done by Linsley (1942) [4] when he saw that the trace from the lower abdomen of his pregnant wife were similar to neonates EEG. The direct measurement from fetal scalp by using special electrodes through the vaginal fornicate had done by Berbstine et al (1955) but first practical continues recordings achieved by suction electrodes by Rosen and Scibetta [5] in 1972. Several studies had been done by using suction/screw electrodes in last decades. However, the fetal EEG recording still is far from clinical procedure like fetal heart rate monitoring. [6]

The EEG patterns of fetus and neonates differ from adults and hence the different frequency band which are explained before cannot use. The EEG recording from normal fetus shows four different patterns; Low Voltage Irregular (LVI), HVS, mixed and trace of alternant. On the other hand, voltage depression and isoelectric patterns are the abnormal FFEG patterns. These patterns are somehow similar to patterns observed in neonate of the same conceptual age. The characteristics of fetal EEG patterns are summarized in Table 2.3 [6]

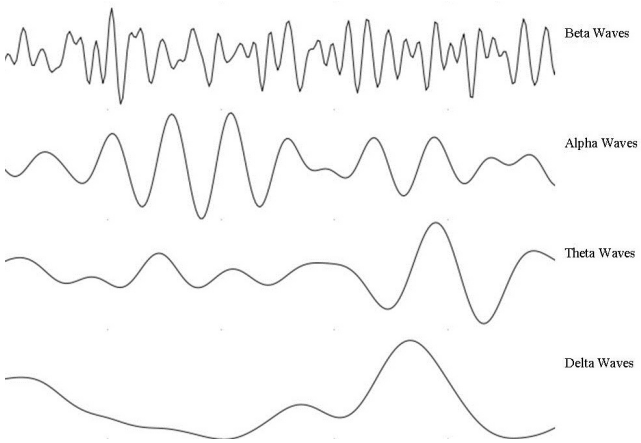

Figure 2.6: The Brainwaves in delta, theta, alpha and beta bands from bottom to top, respectively

Table 2.3: The characteristics of fetal EEG patterns [6]

Pattern	Characteristics	Type
Low Voltage Irregular (LVI)	Continus; dominate by 5-8 Hz frequencies with some slower activity; voltage 14-25 μV	Normal
High Voltage Slow (HVS)	Continues; frequency 0.5-4 Hz; voltage 50-15 μV	Normal
Mixed (M)	ContinuesM HVS intermingled with low voltage fst activity; the voltage is generally lower than that seen in HVS pattern	Normal
Trace alternant (T/A)	Bursts of HVS with occasional superimposed faster low voltage waves; these bursts have duration of 3-8 seconds and are separated by 4-8 seconds of attenuated mixed frequency activity	Normal
Voltage depression	Continues; voltage 5-10 μV; frequency not specifically determined	Abnormal
Isoelectric	Voltage less than 5 μV; frequency not characterized	Abnormal

Burst-suppression

The Burst-suppression (BS) is a pathology pattern in electroencephalogram which can indicate brain damage cause by e.g asphyxia. The asphyxia is related to lack of oxygen and nutrient supply to the brain which can accrue during labor. BS pattern contains important information about prognosis of patient and can be used by clinicians to adjust treatment [7]

It is reported that clear fetal EEG can be obtained more from central and parietal areas than from low occipital or temporal regions. The fetal brain maturation is not same for different regions. Since maturation rate is slower for occipital and temporal regions, these regions are more or less electrically silent. However the precise location of electrodes is not critical when the EEG is used to monitor changes in cerebral activity during time. [6, 8] By the way, the current project aim to provide clear fetal EEG signals to detect burst-suppression patterns and BS is a global phenomenon which is not so sensitive to location.

2.3 Wavelets

2.3.1 Introduction

The fundamental limitation of Fourier transform is the fact that all information about time localization of a given frequency component will be lost in Fourier transform. For instance the power spectrum of a music signal is exactly same as power spectrum of inverse one. The reason of losing this information is the kernel function of Fourier transform, infinite cosine or sine. The windowed Fourier transform is a traditional way to overcome this problem. The windowed Fourier transform is multiplying infinite cosine or sine with a window function, a Gaussian for instance. This window will translate or shift through all signal. This method will provide the frequency information of every segment of signal but will introduce another problem. How choose the size of window? By choosing the very small window to have very good resolution in time domain, the resolution in frequency will be coarse. In the other hand, choosing large window to have good frequency resolution and resolve low frequencies will lead a bad time localization of frequency information. The time frequency resolution of the windowed Fourier transform is constant. [9]

The wavelet transform is a new mathematical tool that can provide a multi-resolution view of the signals. The signal will first analyze in a finest resolution consistent of the data and then at coarser and coarser resolution levels. The wavelet probes the structure of signal and using contribution of different scales. Wavelets are one of state-of-the-art techniques used for noise reduction and compression and analysis in digital signal and image processing. [10]

2.3.2 Wavelet transform

The general linear time-frequency transform can be define as

$$s(t) \mapsto S(a,b) = \int_{-\infty}^{\infty} \psi^*_{ab}(t)s(t)dt \tag{2.1}$$

where
$s(t)$ is the signal
$S(a,b)$ is the transformed signal at scale a and position b
and $\psi^*_{ab}(t)$ is the kernel function

The kernel function of windowed Fourier transform is as equation 2.2 where the a-dependence and b-dependence are modulation and translation, respectively. Therefore the windows $\psi^*_{ab}(t)$ have same width as the $\psi(t)$.

$$\psi^*_{ab}(t) = e^{it/a}\psi(t-b) \tag{2.2}$$

The wavelet transform kernel function is as equation 2.3 where a-dependence is a dilation (a > 1) or contraction (a <1) and the b-dependence is a translation, and hence the wavelets $\psi^*_{ab}(t)$ are self-similar to the $\psi(t)$. The figure 2.7 shows adaptive time-frequency resolution of wavelet compare to fixed time-frequency resolution of windowed Fourier transform.

$$\psi_{ab}(t) = \frac{1}{\sqrt{a}}\psi(\frac{t-b}{a}) \tag{2.3}$$

The wavelet transform in practice is done by decomposing the signal into an approximation and detail. The approximation achieves by low-pass filtering and detail achieves by high-pass filtering. The information contains in detail and approximation is same as the information in the original signal. The decomposition of approximation and detail will continue on the approximation to desired level, the result will be a very rough approximation and series of finest and finest details. The high-pass and low-pass filtering in the decomposition procedure should follow by down sampling; otherwise data will be duplicated during each decomposition. The down sampling will not cause aliasing (loss of information) by using the special "Quadrature mirror filter". This procedure will be very fast because of down sampling and is called fast wavelet transform. The fast wavelet transform is even faster than

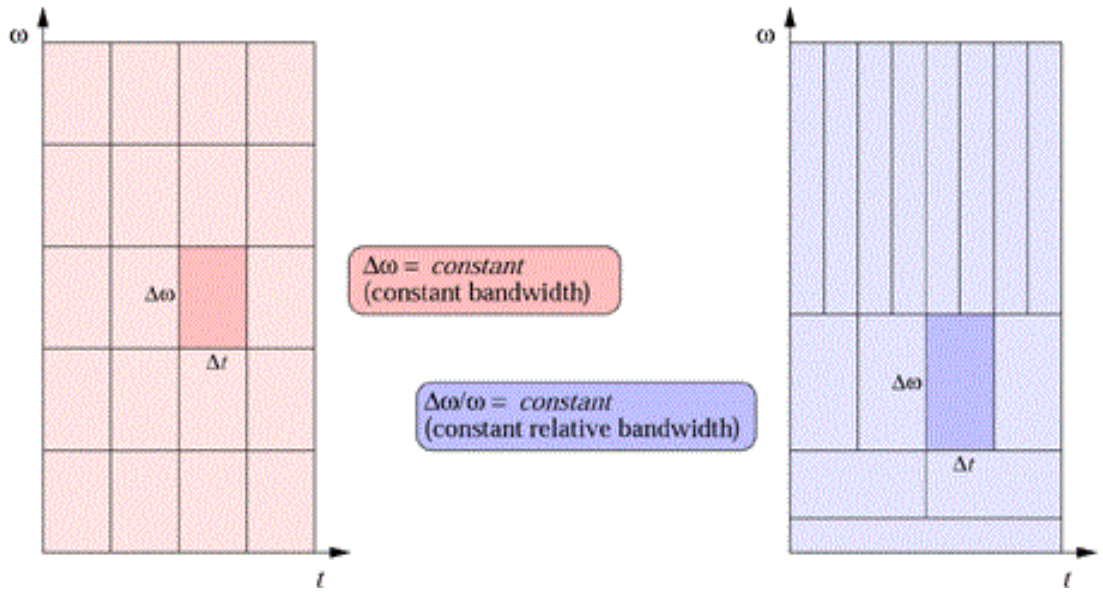

Figure 2.7: The comparison of Time-frequency resolution of windowed Fourier transform to the left and wavelet transform to the right. The $\triangle$ t and $\triangle\omega$ are the time and frequency resolution respectively. The $\triangle t \triangle\omega = constant \geqslant 1/2$ due to Heisenberg uncertainty principle.

fast Fourier transform, its complexity is $4MN$ instead of $2N \log_2 N$ where M is the size of wavelet and N is the size of discrete signal. The procedure of fast wavelet transform and the transformed signal are depicted in figure 2.8 .

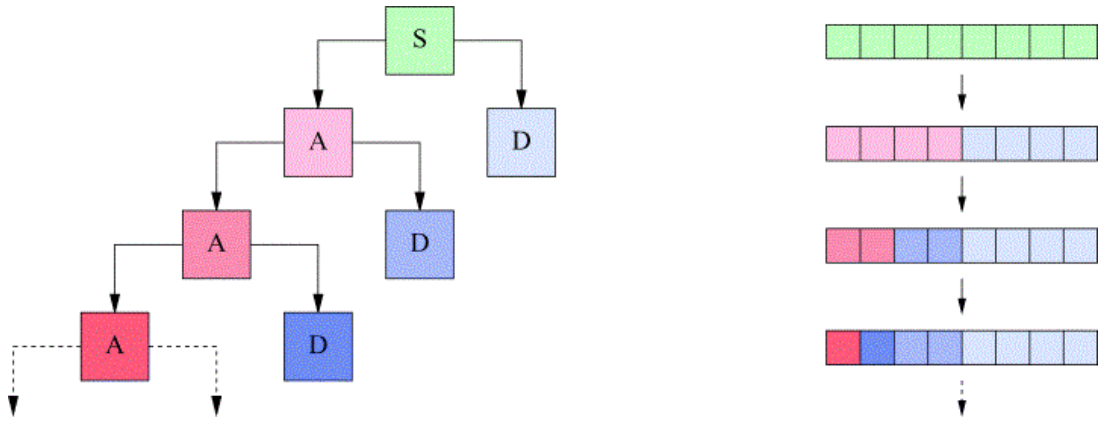

Figure 2.8: The procedure of fast wavelet transform to the left and structure of the transformed signal to the right. The 'S 'is the original signal and 'A' and 'D' are the approximation and details produced by low-pass and high-pass filtering, respectively. The structure of signal shows the effect of down sampling which produce the transformed signal with same length of original signal in each decomposition step.

2.3.3 Wavelets properties

There are dozens of wavelets families exists which provide different analysis functions. There is not a wavelet which with good performance in all applications. There are some conditions can be imposed, so selection of optimal wavelet depends on their properties. The wavelet properties include size of support, symmetry, number of vanishing moments, regularity and orthogonality.

Size of Support

The interval where the wavelet is non-zero is called support. The size of support will influence on the time localization of wavelet as well as speed of transform. The very large support will cause a poor resolution and low speed. Therefore the smaller size of support is desired.

Number of vanishing moment

The wavelet $\psi(x)$ in equation 2.4 has n vanishing moments where x denotes time or space. Since the admissible condition for existence of inverse wavelet transform is to have zero mean, typical wavelets have zero mean $(n = 1)$. The number of vanishing moments effect on frequency localization. The wavelets with more vanishing moments are desired for compression.

$$\int_{-\infty}^{\infty} x^{\nu}\psi(x)dx = 0 \quad for \quad \nu = 0,1,...,n-1 \tag{2.4}$$

Symmetry

The symmetry influences on the quality of time localization. The asymmetric wavelet can be regarded as giving a location with asymmetric error bar.

Orthogonality/Bio-Orthogonality

The orthogonality means the wavelet transform and the inverse wavelet transform are perpendicular to each other. The orthogonal wavelet could be non-symmetry and irregular which are not desired. However, the wavelet without orthogonality will be very slow transform. The solution is bi-orthogonality which means for each wavelet, decomposition set and reconstruction wavelet are perpendicular.

Desired wavelets

The desired wavelet properties could be described as below:

- Good time localization requires small support high symmetry and good frequency
- Good frequency localization needs many vanishing moments and high regularity
- Fast transform need small support and non-orthogonality

On the other hand, the described properties are interrelated. Small support needs relatively few vanishing moments and low regularity while orthogonality causes asymmetry, except for simple wavelets. Therefore, the requirements for desired wavelets cannot fulfill and their relative importance should consider for wavelet selection in each application.

2.3.4 Wavelets families

Several wavelet families are exists which could choose for different applications. The table 2.4 summarize some properties of famous wavelets. Note that in wavelet notations like "db 1", "db" is refer to surname and 1 is number of vanishing moments while bi-orthogonal wavelet notations like "rbio 6.8" the "rbio" shows surname and numbers are refer to vanishing moments for reconstruction and decomposition, respectively. The kernel function of four wavelet family is depicted in figure 2.9.

Table 2.4: Famous wavelet families

Family Name	Members	Wavelet Type
Haar		Orthogonal
Daubechies	db 1, db2 . . . db10	Orthogonal
Coiflets	coif1,coif2,coif3,coif4,coif5	Orthogonal
ReverseBior	rbio1.1,rbio 1.3,rbio 1.5,rbio 2.2,rbio 2.4	Bi-Orthogonal
	rbio 2.6,rbio 2.8,rbio 3.1,rbio 3.3,rbio 3.5	
	rbio 2.6,rbio 2.8,rbio 3.1,rbio 3.3,rbio 3.5	
	rbio 3.7,rbio 3.9,rbio 4.4,rbio 5.5 ,rbio 6.8	

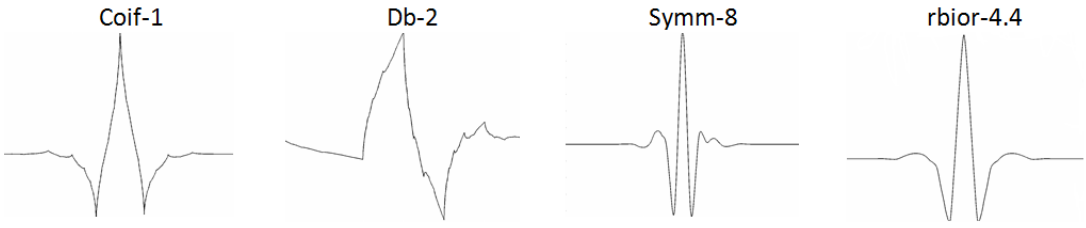

Figure 2.9: The wavelet kernel function of Coiflet-1, db-2, symm-8 and rbior-4.4 are depicted from left to right

3

Experimental Setup

The current STAN S31 monitor, available channels modification methods, limitations and recording protocol are described in this section.

3.1 Hardware Modification and Available Channels

The STAN S31 monitoring system is using two electrodes. The first electrode is called Goldtrace ECG scalp electrode as shown in figure 3.1. The Goldtrace ECG electrode consists of spiral electrode and reference hub; as it is obvious in center picture in figure 3.1; the spiral electrode will connect to fetus skull while the reference hub is inside uterus amniotic fluid. The measuring signal from skull electrode is referenced by reference hub and mother thigh skin electrodes to achieve Fetal Heart Rate (FHR) and fetal Electrocardiogram (fECG), respectively.

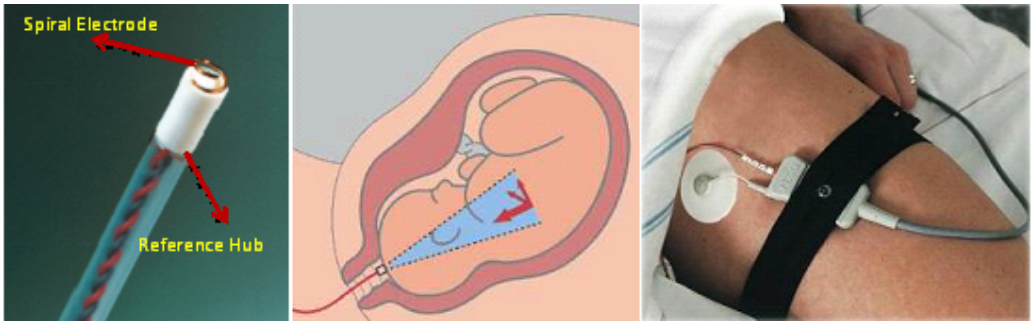

Figure 3.1: The picture shows the Goldtrace ECG scalp electrode, placement of scalp electrode and mother thigh skin electrode from left to right, respectively.

The specification of available channels are summarized in table 3.1. The STAN S31 uses a 12 bit Analogue to Digital Converter (ADC) which admits a resolution of 5 μV. This resolution is sufficient for Heart Rate and ST analysis but for EEG measurement the 1 μV resolution is needed.

The modification for achieving higher amplitude resolution can be done by using 18 or 24 bit ADC or by higher amplification of signals before ADC. The modification on experimental prototype amplifier should not interference with current clinical usage of STAN on hospital. Therefore, the amplification of signals and using the MECG channels which is not currently used in Möndal Hospital, have chosen.
Since only one channel is available for modification, either FHR or ECG channel can redirect to the MECG channel after amplification. The FHR channel is selected because of initiate idea that FHR channel could contain more EEG content.

The ECG amplifier of STAN S31 consists of several analogue filters and Non-Inverting amplifier. The example Non-Inverting amplifier is illustrated in figure 3.2 . The gain of this kind of amplifier can

Table 3.1: Specification of available channels in STAN S31

Name	Derivation	Frequency Range (Hz)	Sampling Frequency (Hz)	Clinical Usage
FHR	Spiral - Reference Hub	2-45 Hz	500	Fetal Heart Rate Monitoring
FECG	Spiral - Mother Thigh	0.5-45 Hz	500	Fetal ECG processing (ST Events)
MECG	Mother Thigh - Reference Hub	2-45 Hz	500	Mother Heart Rate Monitoring
UA	—	—	10	Monitoring of Uterine Activity

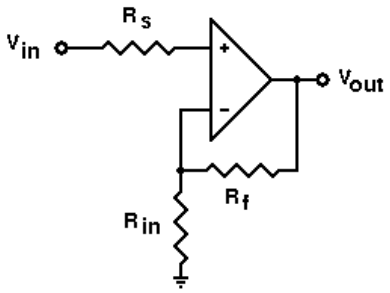

Figure 3.2: The picture shows the Schematic Diagram of Non-inverting amplifier

calculate by using equation 3.1

$$A_v = 1 + \frac{R_f}{R_i n} \tag{3.1}$$

The schematic diagram of amplifier before ADC is depicted in figure 3.3. The modified parts can distinguish by red boxes and consist of changing the resistor R235 to 1.24 $K\omega$, removing C175 and make short cut instead of C62. The verification tests by using ECG signal generator had been done to validate the system. Finally, the medical safety tests had been done by safety department of Neoventa.

3.2 Frequency Challenges

The low frequency components are very sensitive to the motion artifacts. STAN S31 is designed for ECG analysis during labor which is an unstable condition and mother motion and uterine contractions will produce an unstable baseline which is not desired. Currently analogue bandpass filters of 2-45 Hz and 0.5-45 Hz are implemented to reduce an stable baseline (see table 3.1). During the progress of project it has found that the digital comb filter for removing power line disturbance is implemented in DSP and is applied to MECG channel. Unfortunately, implemented comb filter also works as high pass filter with cut of frequency 5 Hz and hence most of desired frequency range for fetal EEG analysis is not accessible in this channel. The modification of this filter in DSP needs more study to be sure about clinical influences which is not include in scope of current project. The frequency response of comb filter can be found in the Appendix A.2.

3.3 Recording Protocol

The recordings have been done in delivery department of Sahlgrenska University Hospital, Mölndal by supervision of Ann Santesso. The raw data have recorded on remote server in hospital network, while the signals for ST-Events stored locally in STAN. The gestational age, birth weight, apgar score, drugs or medications during pregnancy, drugs or medications before or during labor and estimated place of electrode on scalp have recognized as interesting parameters which are included in recording protocol as you can see in Data-Acquisition in appendix A.1 .

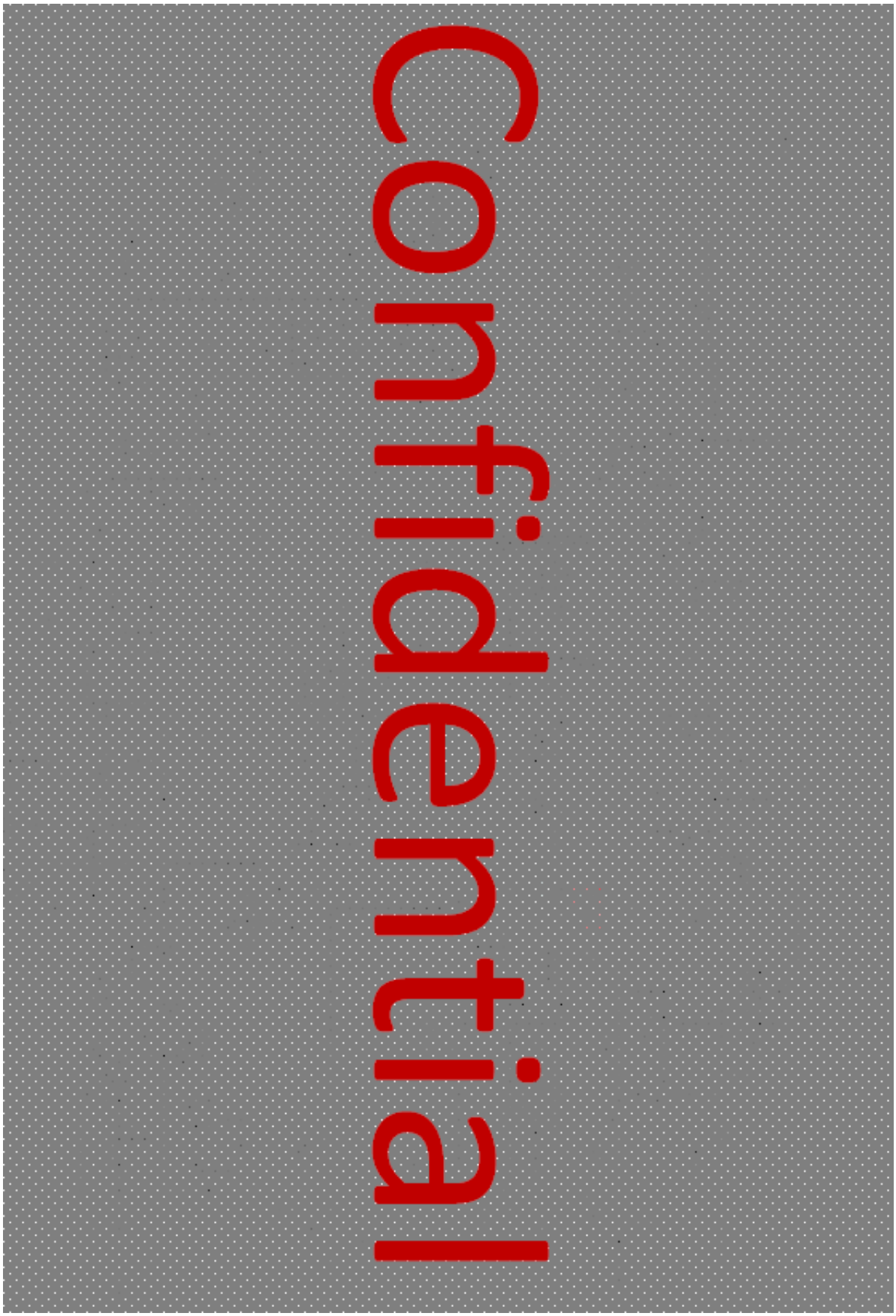

Figure 3.3: The picture shows the Schematic Diagram of STAN S31 Amplifier before ADC. The red boxes are depicting Modified parts.

4

Methods

The recording signals from fetus skull obviously contain heart rate of fetus and even mother heart rate can be distinguished some times. The current usage of signals in STAN S31 is for monitoring of Heart Rate and ECG analysis. Therefore, the ECG is considered as main signals and other signals such as brain and muscle activities are noise which should be eliminated as much as possible during analysis. In contrast, in this project the interested signal is brain activities which considered as noise before. The elimination of noises can achieve by several single or multiple channels methods like Independent Component Analysis, Adaptive filtering, Kalman Filtering, Wavelet denoising, digital filters and ensemble average subtraction. [11]

The simple digital high pass, low pass or band pass filters cannot use for rejection of ECG signals because of their shared frequency range. On the other hand, the limitation of having one channel with high resolution in current project, make the multichannel filtering methods not applicable. Therefore, Ensemble Average Subtraction (EAS) and wavelet denoising are implemented in this project. This chapter consists of description about implemented preprocessing and ECG noise reduction methods.

4.1 Preprocessing

The power-line interference is a common noise source in any bioelectrical signal recordings. This noise is characterized by 50 or 60 Hz sinusoidal interference and can accompany by number of harmonics. The 50 Hz multinotch FIR filter is designed to remove powerline interference. The magnitude response of designed filter is depicted in figure 4.1. [12]

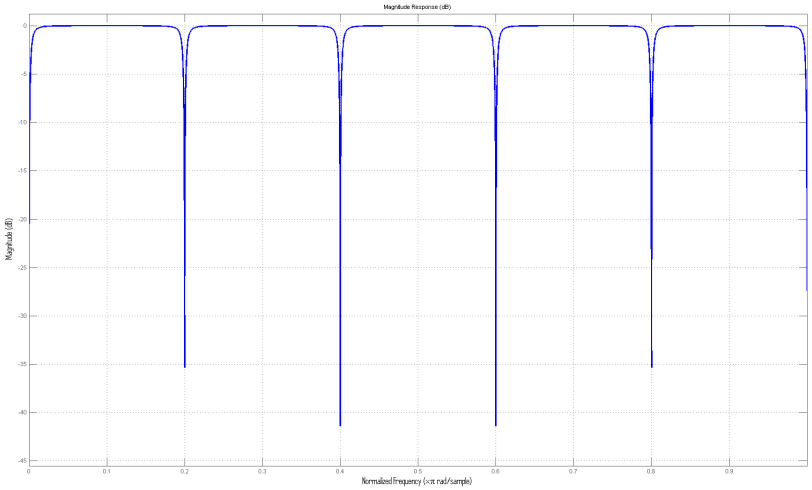

Figure 4.1: Magnitude response of used Comb Filter for removing power line interference

4.2 Ensemble Average Subtraction Method

The ensemble averaging method for elimination of ECG artifacts from EEG signals is introduced by Nakamura [13]. The elimination method consists of R-Peak detection, partitioning of signal to PQRST segments, averaging the segment and subtract the average from each segment. The elimination procedure is depicted in figure 4.2 and described here.

- ***Synchronized partitioning***

  The recorded signal is assumed to be sum of the EEG $x(t)$ and ECG artifacts $z(t)$ as equation 4.1.

  $$y(t) = x(t) + z(t) \tag{4.1}$$

  The R-Peaks of ECG are used as trigger points. The beginning of PQRST segments in original method are set to 200 msec before the trigger point. Then, raw signal partitions into segments as y_j* in equation 4.4.

  $$y_j^*(\tau + t_j) = y(\tau + t_j)\{u(\tau) - u(\tau + t_j - t_{j+1})\} \tag{4.2}$$

- ***Averaging***

  The achieved signal segments are averaged as below:

  $$\bar{z}^*(\tau) = \frac{1}{L_\tau} \sum_{j=1}^{L} y_j^*(\tau + t_j) \tag{4.3}$$

  The synchronous components z(t) like ECG artifacts, become evident in proportion of averaged segments. On the other hand, asynchronous components x(t) will decrease gradually.

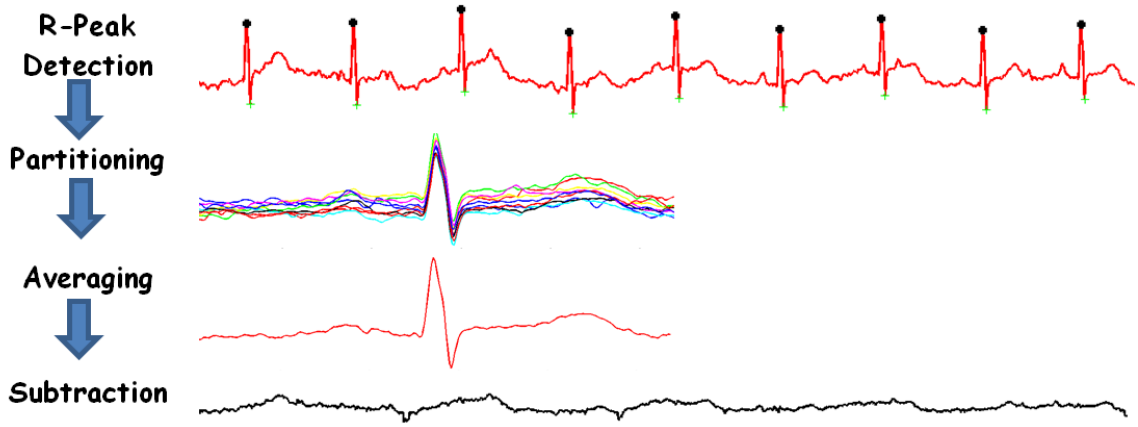

Figure 4.2: Procedure of ensemble averaging method, R-Peak detection, synchronous partitioning, averaging and subtraction

- *Subtraction*

  The average of segments is used as estimate of artifacts z(t). The processed EEG signal ($\hat{x}(t)$) is obtained by subtracting the estimated artifact from the raw signal y(t), as follow equation 4.4.

$$\hat{x}(t) = y(t) - \bar{z}(t) \tag{4.4}$$

The selection of number of segments which should average will influence estimated artifact. The usage of long averaging fragments will destroy some interference details, while very short signal cannot separate the artifact from the underlying signal. Duration of fragmented signal have chosen to 10 second by visual observation.

Modifications are made to the original EAS method. First, by using weighted average and giving double weight to the R-Peak which should eliminate in the signal. Second, using median instead of average to remove outliers from averaging procedure.

4.2.1 QRS and Heartrate Detection

The accurate R-Peak detection which uses in synchronous signal partitioning of ensemble average method is critical for performance of algorithm. The QRS detection can be challenging due to physiological variability of QRS complexes as well as presence of noises. Typical noises include muscle noise, electrode motion, baseline wander and T waves with high-frequency characteristics similar to QRS complexes. [14] The QRS detection algorithms had been under research for more than 30 years. During these decades different approaches based on derivate, digital filters, wavelets, neural network, genetic algorithm are introduced. [15]

The old fashion derivate based algorithm which is introduced by jiapu pan [14] is chose in this project. Modifications are made during implementation to achieve better performance. The processing steps of QRS detection algorithm is depicted in figure 4.3 and described in following.

Figure 4.3: Processing steps of QRS detection; includes linear processes band-pass filter, a derivative and a moving windows integrator and nonlinear transformation squaring and adaptive thresholds.

- ***Bandpass Filter***

  The frequency components of a QRS complex typically range from about 10 Hz to about 25 Hz. The derivative function will amplify high frequency noises. Therefore, it is desired to use digital filters to attenuate other signal components and artifacts like muscle noise, baseline wander, T-wave interference and in-coupling noise. The attenuation of the P and T waves and base line drift requires high-pass filtering while removing in-coupling noises needs low-pass filter. It could practical to use a band-pass filter or cascading low-pass and high-pass filters according to implementation requirements. The desired passband to maximize the QRS energy is approximately 5-15 Hz in the original method. However, in practice, the 5-30 Hz band-pass filter is used in this project. The differences between raw and band-passed signals are depicted in figure 4.4.

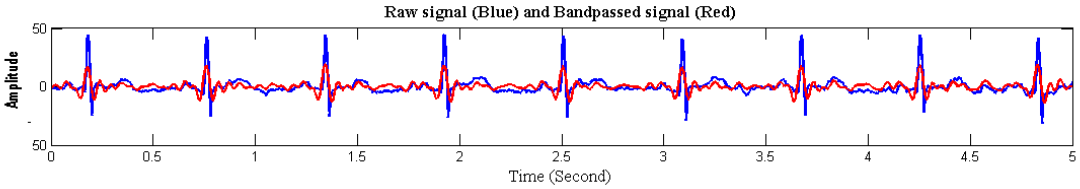

Figure 4.4: Raw signal vs. Band-passed signal; The reduction of low and high frequencies is obvious.

- ***Derivative***

  The QRS slope information can calculate by differentiation of signal.

- ***Squaring Function***

  The differentiated signal is squared point by point as equation 4.5.

$$y(nT) = [x(nT)]^2 \tag{4.5}$$

  The squaring makes all points positive and does nonlinear amplification of derivative's output which emphases higher frequency components. The differentiated and squared signal are depicted in figure 4.5.

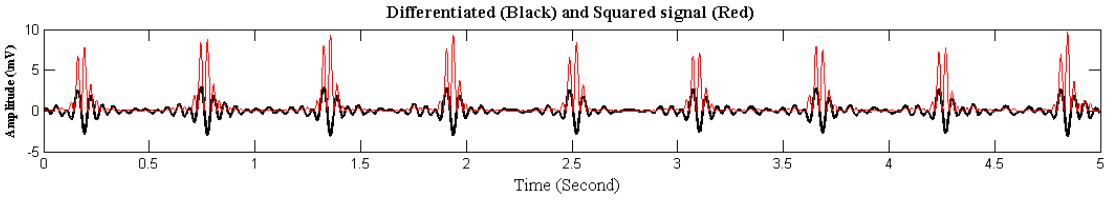

Figure 4.5: The differentiated and squared signal are depicted with black and red, respectively. It is obvious that all points are nonlinearly amplified.

- ***Moving Average Integration***

  The waveform feature information in addition to slope of R wave is calculating by moving-window integration as equation 4.6.

$$y(nT) = (1/N)[x(nT-(N-1)T) + x(nT-(N-2)T) + ... + x(nT)] \tag{4.6}$$

  The moving window length N is important; it approximately should be same as the widest possible QRS complex. The too wide window will merge the QRS and T complexes together. On the other hand, the too narrow moving window will produce several peaks in QRS complexes. The 150 ms window (75 samples for 500 Hz second sample rate) is determined empirically.

- ***Fiducial Mark***

  The QRS complex corresponds to the rising edge of the integrated waveform. The width of QRS complex is equal to duration of rising edge. A fiducial mark for the temporal location of the QRS can define between rising and falling part of integrated waveform. The proper threshold is important for finding QRS boundaries. The JIAPU Pan method includes several thresholds adjustments which needs for real-time application. Since the real-time application is not important in this project, the threshold simply can define as $Thresh = 0.2 * max(integratedsignal)$. The next step is to make selection pulse compare to the threshold. The left and right boundaries will assign to the rising and falling edges, respectively. The integrated signal by using moving average window and detected boundaries are depicted in figure 4.6.

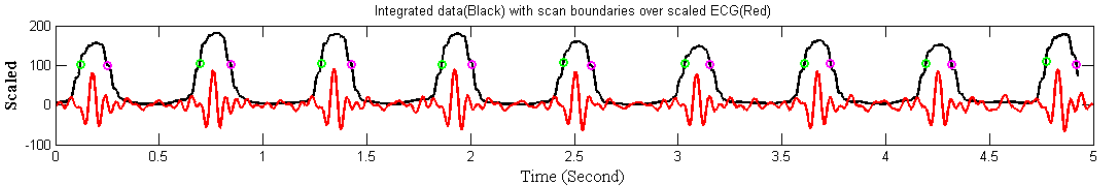

Figure 4.6: The integrated signal over ECG signal and detected QRS boundaries

- ***Decision Rules*** The next step after selecting proper QRS boundaries is to find correspond points for Q, R and S. The decision rules for finding the point can define as follow.

  - ***R-peak*** can simply define as maximum peak between boundaries.
  - ***Q-point*** can simply define as minimum peak between left boundary and R-peak.
  - ***S-point*** can simply define as minimum peak between R-peak and right boundary.

  The algorithm could fail to find some QRS or find some high frequency T-Waves as R-peak. The problem can reduce by using time thresholds between R-peaks to find missed or extra beats. The following rules are applied.

  - The refractory period between two QRS is 200 ms. Therefore, new R-peak cannot be closer than 200 ms to previous one.
  - If the QRS is detected after refractory period but within 360 ms of previous one, It should examine if it is valid QRS or a T-wave. The waveform with largest slope can consider as QRS complex.
  - If the QRS does not find during 166 percent of average RR time, the QRS is missed and the maximum peak between two QRS should examine to see if it is a QRS.

  The detected QRS complexes and RR time intervals are depicted in figure 4.7.

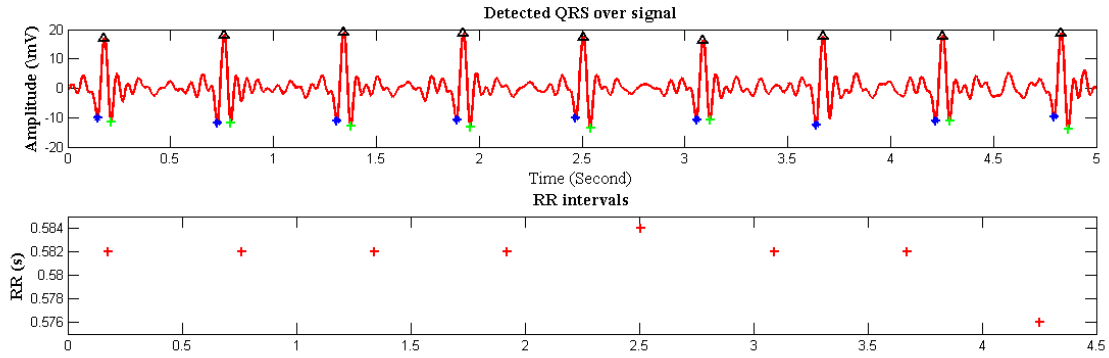

Figure 4.7: The ECG signal and detected R-peaks, Q-points and S-points are shown by triangle(black), star(blue) and plus(green), respectively to the top. The RR intervals in seconds to the bottom

4.3 Wavelets Noise Rejection Method

The simple idea is placed behind wavelet noise rejection method; suppose the signal which contaminated by white noise, ideally non-noisy part of signal get concentrated in a few large coefficients while noise is mapped in a lot of small coefficients. The threshold can consider to set all small coefficients to zero and then reconstructing the signal. The noise rejection steps by using wavelet is depicted in figure 4.8. The proper threshold is critical for good performance of denoising and usually select in an empirical way. The elimination of ECG noises and QRS detection by using wavelets are reported in literatures like Joe-Air Jiang [11] and P.Sasikala [16], respectively.

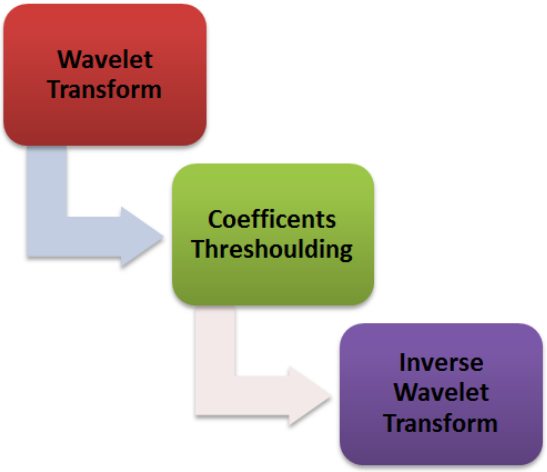

Figure 4.8: Wavelet noise rejection steps

The first step is to select a proper wavelet which has properties and temporal morphology similar to ECG signal. The Coiflet-1, Daub-2 and Symlet-8 are reported in literatures. The Coiflet-1 which have spiky and sharp pattern like ECG and reported by [11] is selected for this project. The implementation had done in MATLAB® Wavelet Toolbox 2011. The figure 4.9 shows eight level decomposition of ten second recorded signal from fetus head by using Coiflet-1 wavelet. The repetitive local maximal in wavelet coefficients which are belong to R-peaks are obvious in first five details (d_1,d_2...d_5). The coefficients larger than selected threshold are set to zero and follows by reconstruction to eliminate ECG artifacts.

The ECG rejection by using wavelets has fundamental difference with usual wavelet denoising meth-

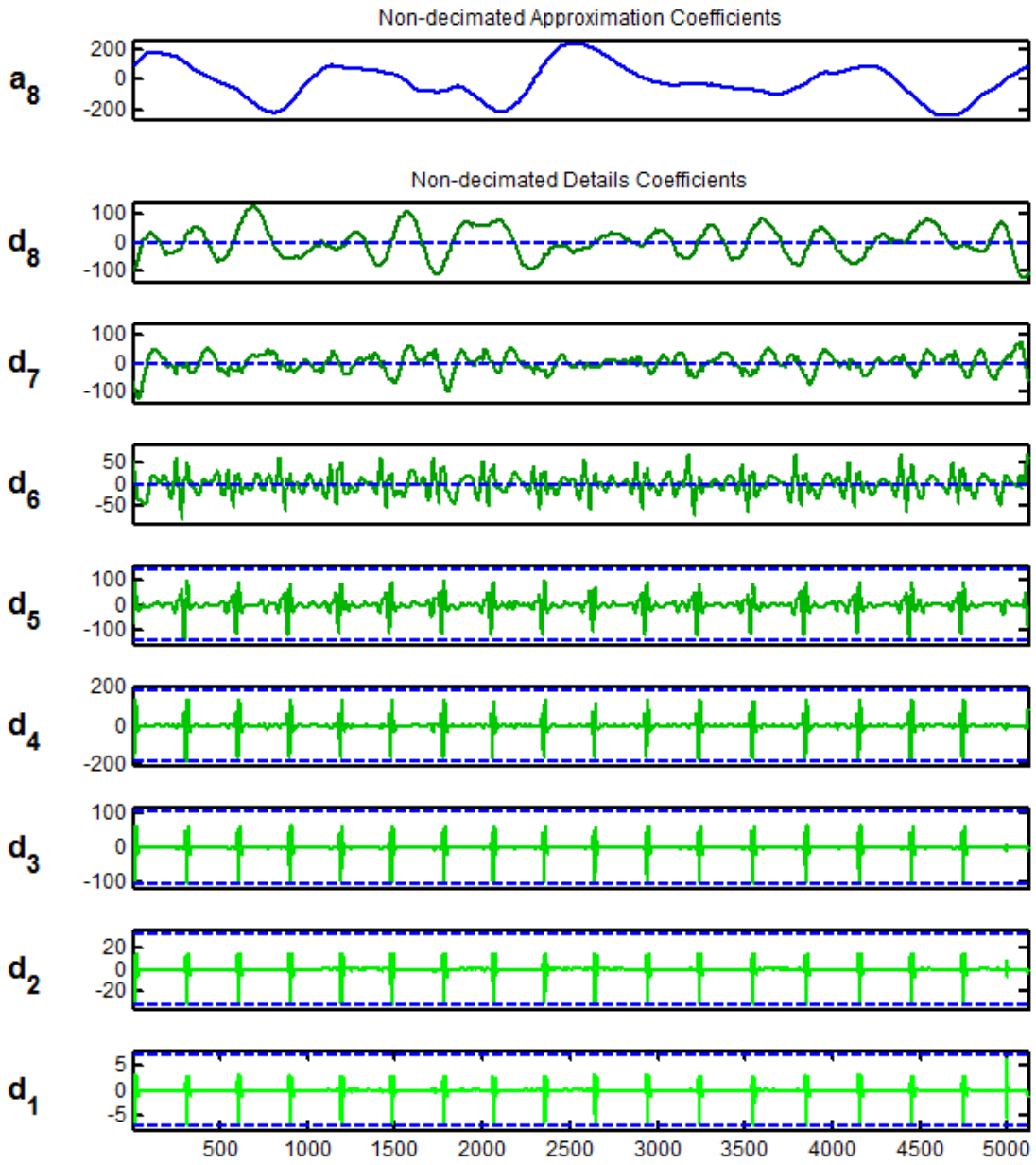

Figure 4.9: Decomposition of 10 second recorded signal from fetus head by using Coiflet-1

ods. The wavelet denoising is based on fact that after wavelet decomposition of noisy signal, the underlying regular part of signal get mostly concentrated into a few large wavelet coefficients while noise is mostly spread into many small wavelet coefficients. Therefore, by selecting a proper threshold all of small coefficients can set to zero and by reconstruction get signal which is almost without noise. In the current case, the large coefficients belongs to the QRS complexes which consider as noise and hence direct use of wavelet denoising module of Wavelet Toolbox is conceptually different. In order to direct using of wavelet denoising module, the threshold should be set as high as possible for details ($d_1, d_2 ... d_5$) which will remove all of details and high frequency components. The modification have made in thresholding to only filter coefficients higher than certain levels. The thresholds are selected by try and error.

4.4 Comparison of methods with simulated signals

The comparison of ECG noise reduction with wavelets and ensemble average subtraction methods can done by applying them to the simulated signals. Since the actual signal is identified, it is possible to compare performance of methods in ECG elimination. The simulation is done by adding ECG noise to the known EEG from neonates and then applying ECG elimination methods to it. The sample of about 10 second EEG from healthy neonate, during quiet wakefulness and its correspond simulated contaminated with ECG noise are depicted in figure 4.10.

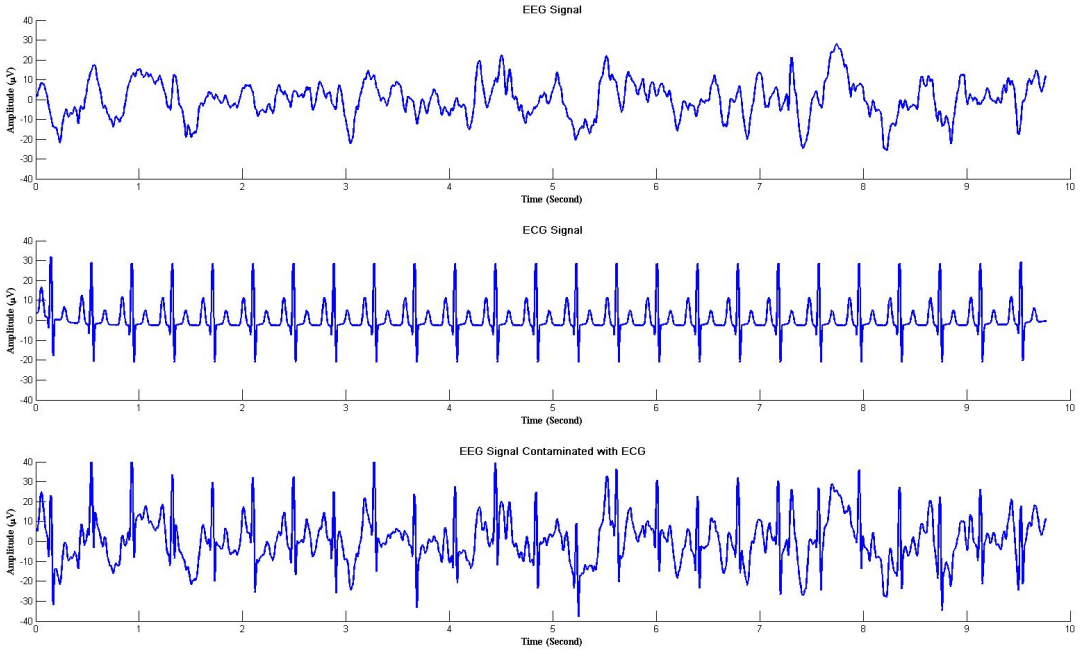

Figure 4.10: The original EEG signal, ECG signal and EEG contaminated with ECG noise from top to bottom, respectively

4.5 Visual Analysis

The visual analysis of recorded and ECG eliminated signals had been done by Dr. Magnus Thordstein at Sahlgrenska university hospital. The signals are exported to European Data Format (EDF) which usually can import to any desired software for interpretation. However, the EDFbrowser [17]; a free and open source viewer for EDF files; have used for browsing and visual analysis of signals. The screen-shot of EDFbrowser is depicted in figure 4.11.

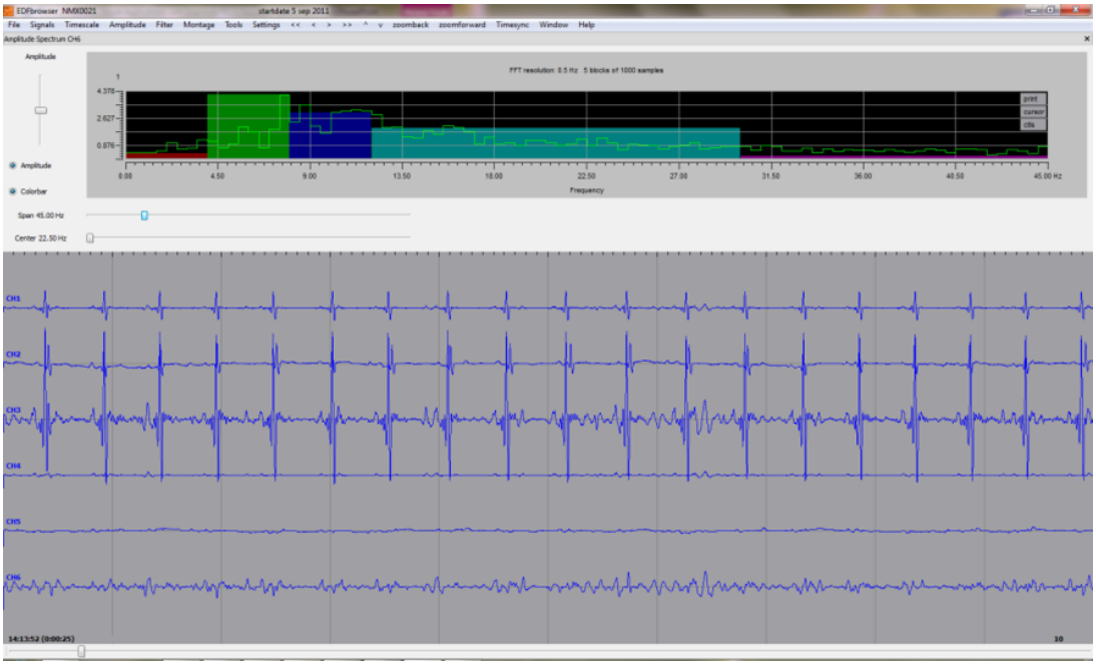

Figure 4.11: Screenshot of EDFbrowser

5

Results

The registered signals and results of ECG elimination methods as well as comparison between them in time and frequency domain is summarized here.

5.1 Recorded signals

After some initial recordings to establish hardware modifications, the signals obtained from five pregnant women who had spontaneous uterine contractions and admitted to the delivery department in Mölndal University Hospital. All subjects had uneventful delivery except one which had ST events. Anyway all deliveries had normal outcome. The registered information of all deliveries is summarized in Table 5.1.

5.2 Ensemble Averaging Subtraction Method

The recorded signal from ECG channel which contaminated with ECG and result of ECG rejection by using ensemble average denoising method is depicted in figure 5.1. The signal has ten seconds length and is selected from subject NMX0088. It is obvious that some QRS complexes are still visible.

5.3 Wavelet Denoising Method

The recorded signal from ECG channel which contaminated with ECG and result of ECG rejection by using wavelet denoising method is depicted in figure 5.2. The recorded signal is the same signal which is used in section 5.3 . It is clear that QRS complex of ECG noise is completely removed.

The figure 5.3 shows the difference between reconstructed signal with Wavelet Toolbox denoising and modified thresholding; it is obvious that the Wavelet Toolbox method gives smoother signal because all the small coefficients in details (d_1,d_2...d_5) sets to zero.

5.4 Comparison of Methods

5.4.1 Simulated Signals

As it is mentioned in methods, comparison had done by using simulated EEG signals contaminated by noise, as well as real signals recorded by modified STAN 31 from fetus scalp. The results of ECG elimination of simulated signals is depicted in figure 5.4. The thirty seconds signal from a healthy neonate, during quiet wakefulness, is selected and contaminated by ECG noise as shown in the plots. The implemented ensemble average subtraction and wavelet denoising methods are applied to the noisy signal

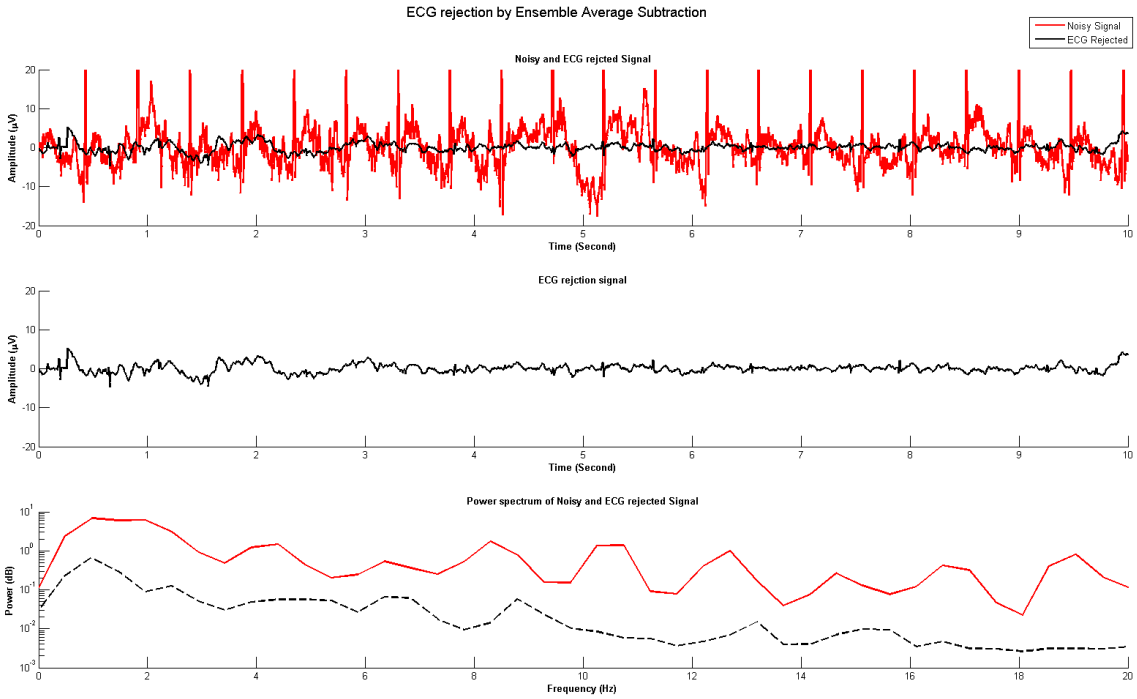

Figure 5.1: The ECG elimination by using Ensemble Average Subtraction Denoising method.

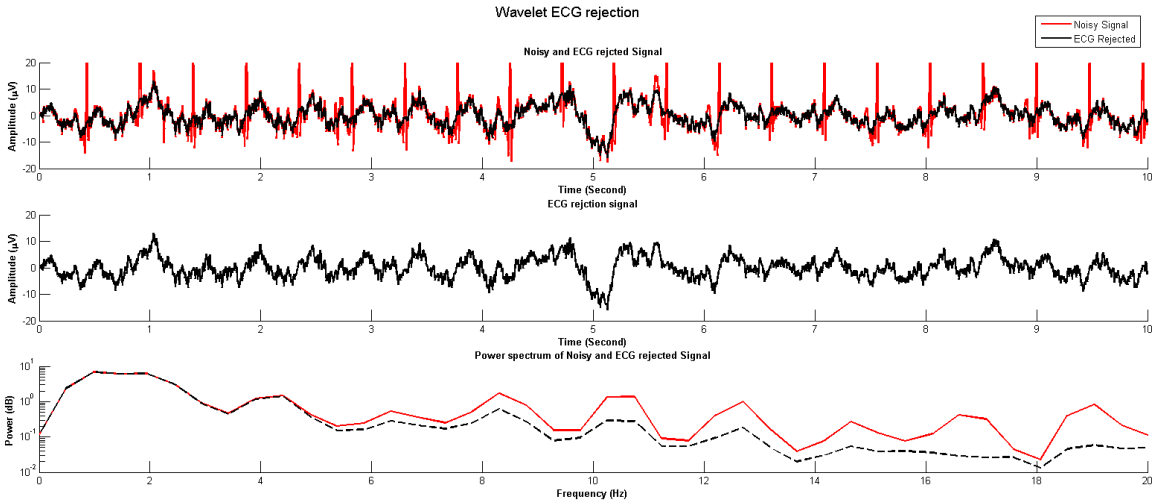

Figure 5.2: The ECG elimination by using Wavelet Denoising method

Table 5.1: Registered information of recordings

Registration Number	Recording Time (minutes)	Outcome	Special Events
NMX0088	118	Normal	ST Events
NMX0139	97	Normal	
NMX0140	77	Normal	
NMX0141	95	Normal	
NMX0144	104	Normal	

and results are illustrated in plots. It is obvious that even both signals almost successfully eliminated noises; achieved signals are not identical.

The time and frequency domain comparison of methods is depicted in figure 5.5. It demonstrates that signal which is eliminated by using wavelet denosing method follows better the morphology and frequency content of original signal.

5.4.2 Real Signals

The results of ECG elimination of real recorded signal are depicted in figure 5.6. The plot contains 10 second signal from Subject NMX0088, which is registered by fECG channel (Spiral Electrode-Mother Thigh). The ECG is almost successfully eliminated by both method; anyway, some remaining part of QRS complexes still visible in ensemble average subtraction method. In the frequency domain, the low frequency power of signal achieved by using wavelet denoising is more than ensemble averaging and it is compatible with result from simulated signals.

5.5 Visual Analysis

The ECG rejected signals have exported to EDF files and visual analysis had done by using EDFBrowser. The results of visual analysis are summarized here.

1. Signals which are eliminated by ensemble averaging subtraction method, still contains some visible QRS complexes.
2. Signals which are eliminated by ensemble averaging subtraction method, contains more low frequency components than signals which are filtered by wavelet denoising.
3. The ensemble average and wavelet methods functions like low-pass and high-pass filters, respectively.
4. Interpretation of ECG eliminated signals for subject NMX0088 which include ST events does not show correlation with any time or frequency event in signals.
5. An unexpected non-biological noise of 5 hertz is obvious in some part of filtered signals.

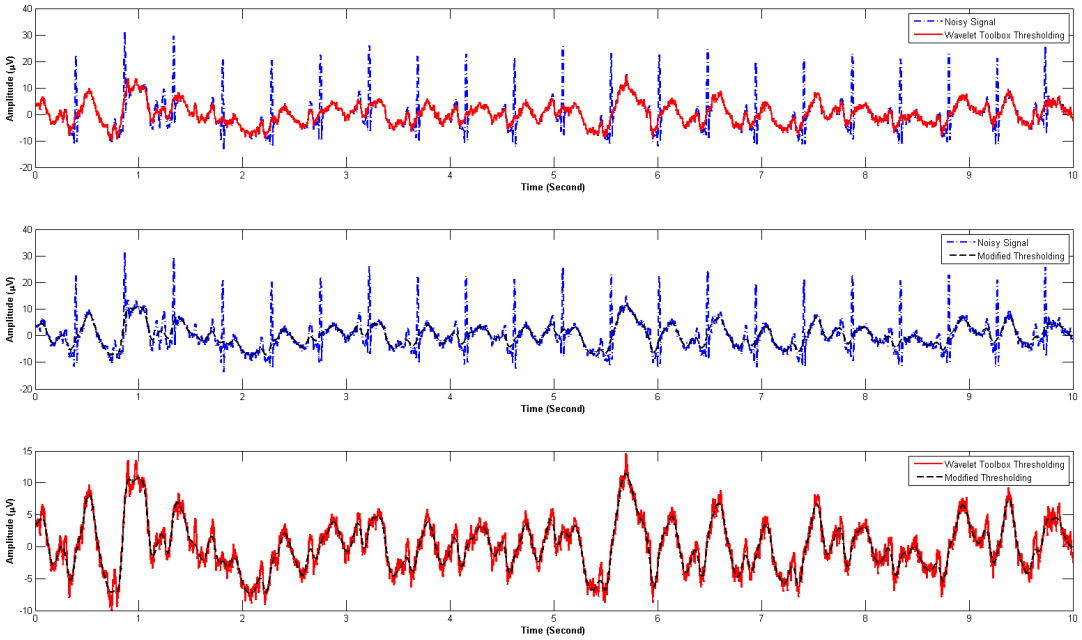

Figure 5.3: The reconstructed signals by using Wavelet Toolbox denoising thresholding Vs. modified version

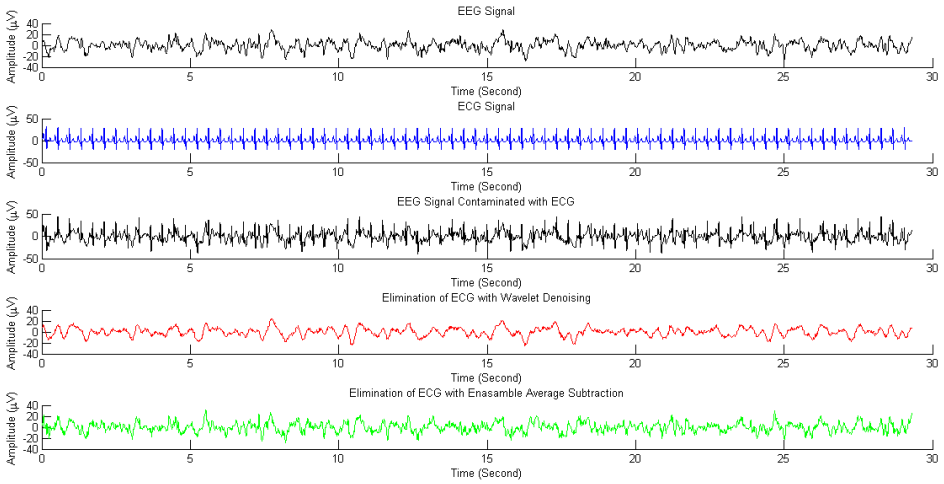

Figure 5.4: The ECG elimination of simulated signal with EAS and Wavelet Denoising methods. The EEG signal from neonate, ECG signal , EEG contaminated with ECG, ECG eliminated with wavelet and ensemble average methods are illustrated from top to bottom, respectively

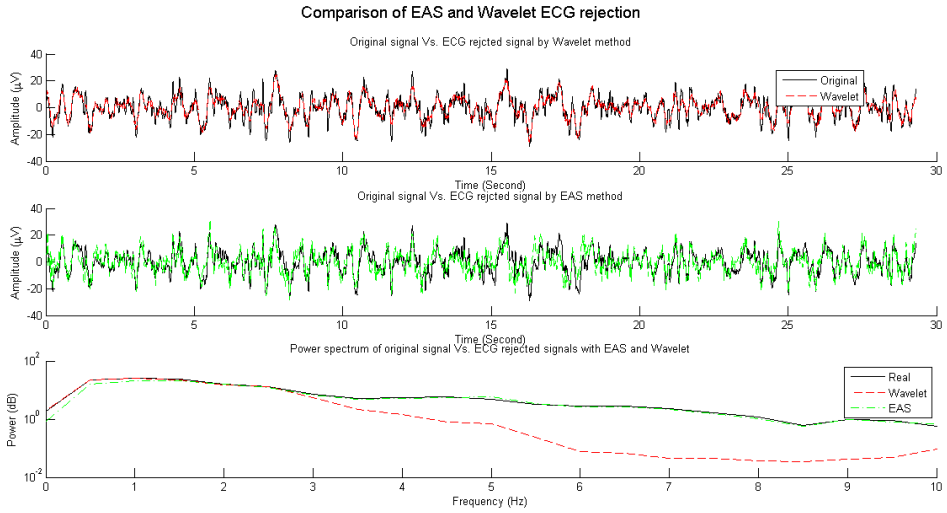

Figure 5.5: Comparison of EAS and Wavelet Denoising methods with simulated noisy signal.

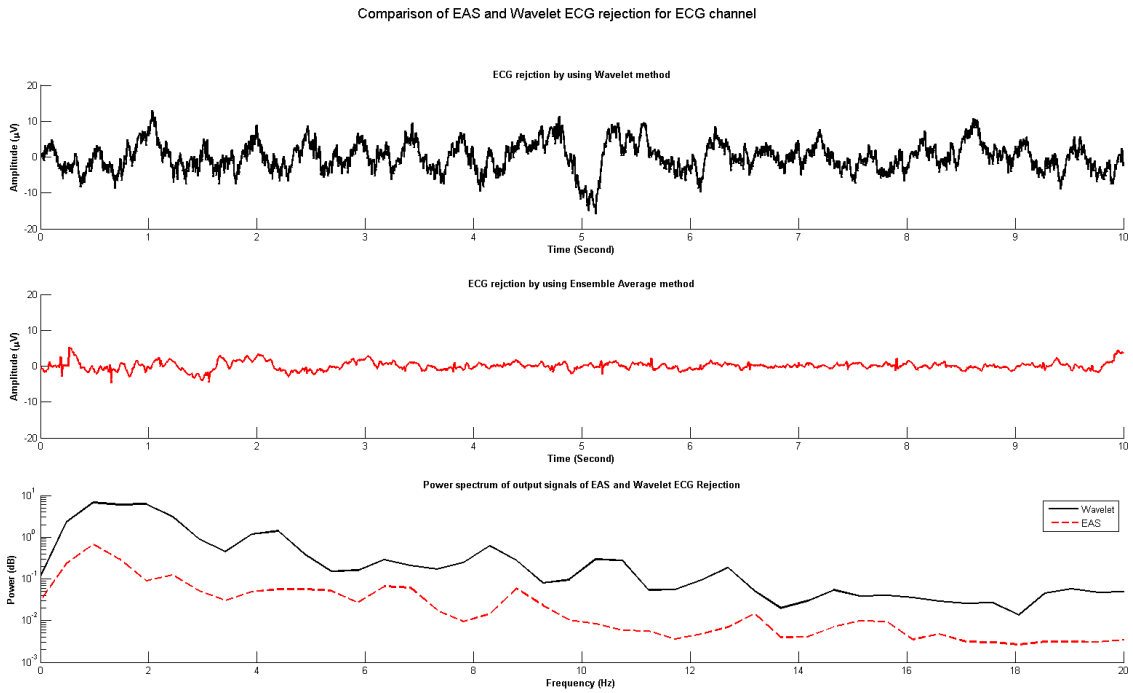

Figure 5.6: Comparison of EAS and Wavelet Denoising methods with real signal from subject NMX008

6

Discussion

The comparison of results of applying implemented methods to simulated signals shows the effect of wavelet denoising method and ensemble average subtraction method as low-pass and high pass filters, respectively. The wavelet denoising method has been done by decomposition of noisy signal to approximation and eight levels of detail. The elimination of QRS is achieved by comparing details coefficients ($d_1, d_2 ... d_5$) with certain threshold and set the large coefficients to zero. Since coefficients in detail are set to zero, smoother signal with lower high frequency components is expected and it operation of this method can consider as low-pass filter. The signal averaging in time domain can consider as smoothing and low-pass filtering. The subtraction of this low-passed signal from noisy signal will produce a high-passed signal and hence ensemble average subtraction method can consider as high-pass filter.

The wavelet denoising method produce a smoother signal which almost none of QRS complexes can be distinguish in the result. On the other hand, results of ensemble average subtraction method show some attenuated QRS which are still visible in the signal. Ideally, the average ECG should be equal to all ECG segments. Anyway, the amplitude of ECG components is variable and several noises are present and hence in reality the average ECG is not same as all PQRST noises. The variety of QRS amplitude remains some visible QRS with low amplitude after subtraction of average ECG from signal. The ensemble average subtraction method is also more sensitive to noise because of noise contribution in the average QRS. We have tried to reduce this sensitivity by using median operation instead of averaging because outliers will not contribute in median.

The technical prospective of comparison of methods for simulated signals, shows wavelet method is more accurate because its output is more follow the real signal. However, the simulated signal is EEG from neonate which contains more low frequency activities and hence this conclusion is not general. We have discussed ideas behind works of wavelet and ensemble average subtraction methods as low-pass and high-pass filter. Therefore, it is not surprising that by using a low-pass filter (wavelet method) in signal with high amount of low frequency components better results can achieve compare to high-pass filter.

The ensemble average method is more accurate in sense that it is estimate different components of ECG like P wave, QRS complex and T wave and subtracts them from noisy signal. Therefore, it is more likely to preserve EEG components which have similar shape and frequency contents of ECG components. The wavelet method on the other hand works blind and will remove details which have shape and frequency contents like ECG components.

The analysis of ensemble average subtraction method output, needs presence of ECG signal as well. The ECG signal can be used to check if a high frequency component is the remaining parts of eliminated QRS. The wavelet method output is interesting because it more preserve low frequencies which are typical components for fetal and newborn babies. From visual analysis perspective, the analysis of low frequencies is difficult and hence output of ensemble average method more suitable for visual analysis.

It can conclude that the usage of these methods could differ in automatic and visual analysis.

Does remaining signals contain EEG? The low resolution signals and limited number of eventful recordings make the analysis of remaining signal difficult. Therefore, even signals are similar to EEG signal, final judgment needs improvement in equipment and experimental method.

7

Conclusion

Hardware modification to achieve 1 μV resolution had done but due to some limitations entire desired frequency range is not covered. The wavelet denoising and ensemble averaging subtraction methods are implemented and successfully applied to the recorded signals. Both methods show well result in elimination of ECG in signals. It is also conclude that wavelet denoising method works like low-pass filter while ensemble average subtraction works as high-pass filter. Therefore, selection of one of these methods depends on the application. Anyway, for busrt-suppression detection which have high frequency contents ensemble average subtraction seems more suitable. The remaining signals after elimination of ECG shows patterns like EEG but final judgment needs signals with higher resolution and with whole desired frequency range.

8

Future Work

The future works can be done to make a final judgment about existence of EEG in the signals which picks up from fetus scalp during labor. The suggested future works are summarized as following.

1. Modification of DSP filters to have high resolution signal in frequency range of 0.5-45 Hz.
2. Design a new experimental setup includes producing somatosensory evoke potential to examine in EEG signals, displacement of mother thigh skin electrode to produce higher quality signal and probably putting two spiral electrodes on the scalp.
3. Obtain necessary ethical approvals.
4. Implementation of other denoising methods like Independent Components Analysis (ICA).
5. Implementing Machine Learning methods in order to find corresponding EEG features with ST events in ECG.
6. Investigating possibility of burst-suppression detection in fetal EEG signals.

References

[1] R. Sameni, G. Clifford, A review of fetal ecg signal processing issues and promising directions, Open Pacing Electrophysiol Ther J 3 (2010) 2.

[2] E. Widmaier, H. Raff, K. Strang, Vander's Human Physiology: the mechanisms of body function, McGraw-Hill Higher Education, 2004.

[3] M. Neuman, Medical instrumentation application and design, New York: J. Wiley and Sons (1998) 233–286.

[4] D. Lindsley, Heart and brain potentials of human fetuses in utero, The American Journal of Psychology 55 (3) (1942) 412–416.

[5] M. ROSEN, On the foetal eeg during parturition, in: Foetal and neonatal physiology: proceedings of the Sir Joseph Barcroft Centenary Symposium held at the Physiological Laboratory, Cambridge 25 to 27 July 1972, Cambridge University Press, 1973, p. 71.

[6] D. Viniker, The fetal eeg (detection of oxygen deprivation)., British journal of hospital medicine 22 (5) (1979) 504.

[7] J. Löfhede, The EEG of the neonatal brain: classification of background activity, Göteborg: Chalmers University of Technology, 2009.

[8] M. Rosen, J. Scibetta, L. Chik, A. Borgstedt, An approach to the study of brain damage. the principles of fetal electroencephalography., American journal of obstetrics and gynecology 115 (1) (1973) 37.

[9] A. Romeo, C. Horellou, J. Bergh, A wavelet add-on code for new-generation n-body simulations and data de-noising (jofiluren), Monthly Notices of the Royal Astronomical Society 354 (4) (2004) 1208–1222.

[10] A. Romeo, C. Horellou, J. Bergh, N-body simulations with two-orders-of-magnitude higher performance using wavelets, Monthly Notices of the Royal Astronomical Society 342 (2) (2003) 337–344.

[11] J. Jiang, C. Chao, M. Chiu, R. Lee, C. Tseng, R. Lin, An automatic analysis method for detecting and eliminating ecg artifacts in eeg, Computers in biology and medicine 37 (11) (2007) 1660–1671.

[12] L. Sörnmo, P. Laguna, Bioelectrical signal processing in cardiac and neurological applications. 2005, Elsevier Academic Press.

[13] M. Nakamura, H. Shibasaki, Elimination of ekg artifacts from eeg records: a new method of non-cephalic referential eeg recording, Electroencephalography and clinical neurophysiology 66 (1) (1987) 89–92.

[14] J. Pan, W. Tompkins, A real-time qrs detection algorithm, Biomedical Engineering, IEEE Transactions on (3) (1985) 230–236.

[15] B. Kohler, C. Hennig, R. Orglmeister, The principles of software qrs detection, Engineering in Medicine and Biology Magazine, IEEE 21 (1) (2002) 42–57.

[16] P. Sasikala, R. Wahidabanu, Robust r peak and qrs detection in electrocardiogram using wavelet transform, International Journal of Advanced Computer Science and Applications-IJACSA 1 (6) (2010) 48–53.

[17] Edfbrowser, leiden university medical centre, netherland (2011).
URL `http://www.teuniz.net/edfbrowser/`

A

Appendix

A.1 Appendix1-Registration Form

Registrering med förbättrad signalupplösning

Födelse (datum, klockslag):

Registreringsnummer:

Kön:

Gestationsålder:

Födelsevikt:

Apgar:

Blodgaser:

Medicinering under graviditet (preparat, dos):

Medicinering i anslutning till förlossning (preparat, dos, klockslag):

Placering av skalpelektrod (markera med X):

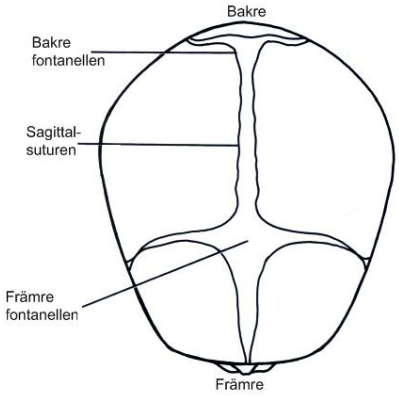

Kommentar:

A.2 Appendix2-Digital Comb Filter

9.6 Cmdinter.asm

Purpose:
Interpret control commands.

Description:
Called from receiveInterrupt when the address information nibble is interpreted to be a control command.
Command word should be in Accumulator A b11-b8. Depending of the information of the command word, different actions are taken.
All environmental variables controlled by the SBC are set in this routine.

9.7 Filters.asm

Purpose:
Include filter files (xx.tab) which are being used in more than 1 filter module.

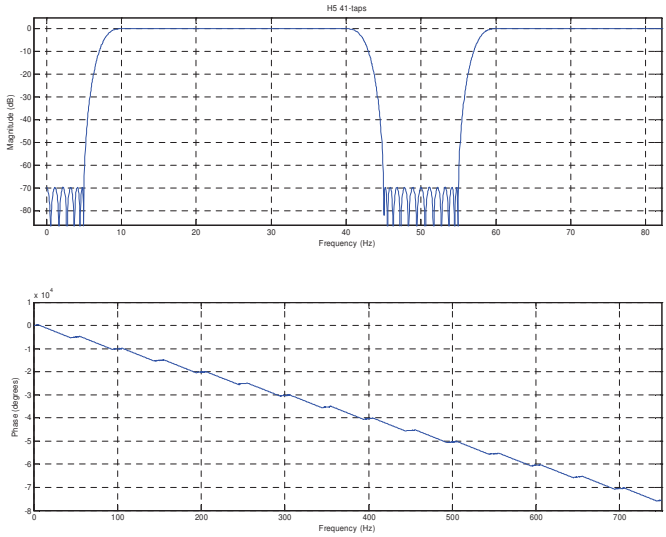

Figure 1. H5 filter response (50Hz multinotch, group delay 204.8 samples @500Hz)

Matlab filter coefficient generation:
1 = 40;
k1 = 30;
F = 0:1/(N1-1):1;
h01 = remez(N1, [0 150/750 300/750 1],[0 0 1 1]);
figure(10), freqz(h01,1,16384,1500);